Investigation of the Bandwidth of Resonators for Frequency-Coded Chipless Radio-Frequency Identification Tags

Tong-Yang Jiang
Department of Electronic Engineering
National Taipei University of Technology
Taipei, Taiwan
t105368038@ntut.edu.tw

Fei-Peng Lai
Department of Electronic Engineering
National Taipei University of Technology
Taipei, Taiwan
t106368033@ntut.edu.tw

Yen-Sheng Chen
Department of Electronic Engineering
National Taipei University of Technology
Taipei, Taiwan
yschen@ntut.edu.tw

***Abstract*—Conventional radio-frequency identification (RFID) tags consist of a chip and a printed antenna. As the chip set is manufactured via the fabrication technology of application-specific integrated circuit, the cost of the chip is much higher than that of the antenna. Furthermore, soldering the chip to the antenna requires an additional procedure, so the main cost of an RFID tag comes from the chip. To eliminate this main cost, "chipless RFID" removes the use of a tag chip. Chipless RFID tags encode data by using several electromagnetic resonators, which can be directly printed on paper or plastic films; thus, the cost of chipless tags is reduced to a level as low as barcodes. Nevertheless, in order to increase the capacity of chipless RFID, the resonators are required to depict a narrow bandwidth. Although several resonators have been proposed for this application, the design that leads to the narrowest bandwidth is still inconclusive. In this study, we investigate the bandwidth of twenty-four resonators that have been employed in chipless RFID tags. It is observed that the quarter-wavelength slot, the circular slot and the Hilbert-curve resonators provide a narrowband feature. These resonators have a potential to enable the chipless tag to enhance capacity.**

Keywords—backscattering, internet of things, radio-frequency identification, radar cross section, resonators, sensor network

I. INTRODUCTION

Radio-frequency identification (RFID) has been extensively used in various commercial applications. An RFID system employs a reader and tags, which transfer data through the technique of inductive coupling or backscattering modulation. The technique of inductive coupling depicts a read range that is smaller than dozens of centimeters, and the frequency band includes 125 kHz at the low-frequency (LF) band and 13.56 MHz at the high-frequency (HF) band. In contrast, the technique of backscattering depicts a larger read range that is greater than one meter. The operating frequency band includes the ultra-high-frequency (UHF) band and the very-high-frequency (VHF) band. Although these conventional RFID techniques have been extensively studied, the cost of a tag has been converged and is difficult to be further reduced. In particular, the cost of a UHF tag is about 20 cents in 2017. As the cost of the tag is inversely proportional to the number of tags used, such a high cost limits the extensive usage of RFID technology. To satisfy the requirement of internet of things (IoTs), which depicts billions of interconnected sensors, it is urgent to reduce the cost of the tag.

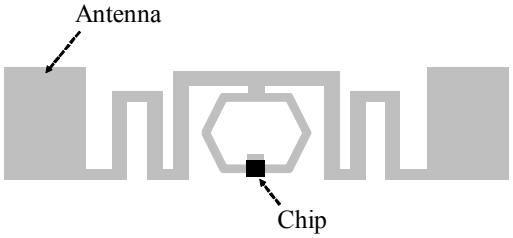

Fig. 1. Illustration of a conventional RFID tag.

The inevitably high cost of the tag is caused by the use of a chip. Fig. 1 depicts the structure of a conventional tag, which comprises a printed antenna and a chip. The fabrication of this tag requires three steps: antenna fabrication, integrated chip (IC) welding and lamination. The antenna fabrication relies on etching, printing or plating. Either option depicts the feature of low cost. In contrast, the IC welding requires an additional procedure such as anisotropic conductive paste, anisotropic conductive film and flip-chip methods. The cost of the IC welding is significantly higher than that of the antenna fabrication. However, the use of the chip is necessary because the information is recorded using the chip. This limitation converges the cost of the conventional tag, and such a high cost is difficult to be reduced unless the usage of the chip can be eliminated.

The RFID technique that eliminates the use of the chip is called "chipless RFID". In fact, several international IoT industries are developing chipless RFID in recent years, although only a relatively expensive chipless technique based on surface acoustic wave has been commercialized [1]. Chipless RFID can be classified into a time-coded [2], frequency-coded [3], phase-coded [4] and hybrid-coded system [5]. Among them, the frequency-coded chipless RFID leads to the lowest cost for the tag fabrication, and it depicts the potential of high capacity. Nevertheless, the frequency-coded chipless RFID faces several challenges that have not yet been overcome. The system architecture, operational frequency, tag design, reader transceiver, design of reader antenna and signal processing of the frequency-coded chipless RFID are completely different from those of the conventional RFID. For

This work was supported by the Ministry of Science and Technology, Taiwan, under Contract MOST 107-2636-E-027-001.

example, the frequency-coded chipless RFID employs electromagnetic (EM) resonators to construct a tag, instead of an antenna with a highly inductive input impedance [6]. In order to implement this technique in real-world applications, more number of studies are required.

This study intends to investigate the topology of the EM resonators that leads to a narrowband characteristic for the chipless tag. Although several resonators have been proposed [7–19] for this application, the topology of the resonator that leads to the narrowest bandwidth is still inconclusive. Only by minimizing the bandwidth can the capacity of the system be enhanced. To this end, the bandwidth of radar cross section (RCS) for twenty-four resonators is evaluated. All the resonators are constructed with single-sided printing so that they can be manufactured straightforwardly and attached to an object. The performance supplemented using CST simulation is demonstrated.

II. Frequency-Coded Chipless RFID

The frequency-coded tag can be classified into a backscatter-based tag [7–16] and a bandpass-filter-based tag [17–19]. The backscatter-based tag consists of several EM resonators. When a broadband EM wave illuminates the tag, some resonators designed at this frequency band function as a radiator, thereby varying the backscattering power. In contrast, the other resonators that are not operated at this band do not influence the backscattering power. Thus, the backscattering power depicts two levels, which can be further encoded as binary data. Fig. 2 shows an example of the backscatter-based tag. The two tags represent "1000" and "1100", respectively. The difference between them is the information relating to the second bit, which is caused by the configuration of a slot. Using two monopole antennas that are designed to operate at 2.0–4.5 GHz, we measure the associated RCS response for the two tags. The measured results are depicted in Fig. 3. As can be observed, the second bit demonstrates two distinct levels, which can be defined as 0 and 1, respectively. Using this technique, previous studies have proposed various topologies for the EM resonator, including circular [7], L-shape [8], dual-polarized stub [9], dipole-segment [10], U-shape [11], dual-rhombic [12], octagonal [13], slot [14], pixel [15] and step-impedance [16] configuration. The operational mechanism of these resonators can be clarified using high impedance surfaces [20] or frequency selective surfaces [21]. Some previous studies focus on the printability of the chipless tag using inkjet printing technology [22]. However, the ultimate objective of these resonators is to depict the resonance with a high quality factor and a narrow bandwidth.

Additionally, the bandpass-filter-based tag employs two orthogonally-polarized antennas interconnected with a bandpass filter [17–19]. The first antenna transmits an impinged signal to the second antenna, and this signal is attenuated by the bandpass filter. Thus, when the second antenna re-radiates the signal back to a reader, the reader can decode the binary data on the tag. The bandpass-filter-based tag can be designed using microwave filter theory. On the other hand, the backscatter-based chipless tag is required to be evaluated using full-wave simulation, which is relatively computationally expensive. However, the bandpass-filter-based tag usually depicts a larger size.

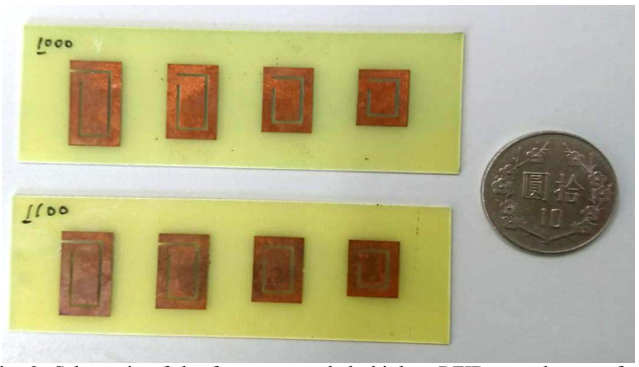

Fig. 2. Schematic of the frequency-coded chipless RFID tags that use four EM resonators.

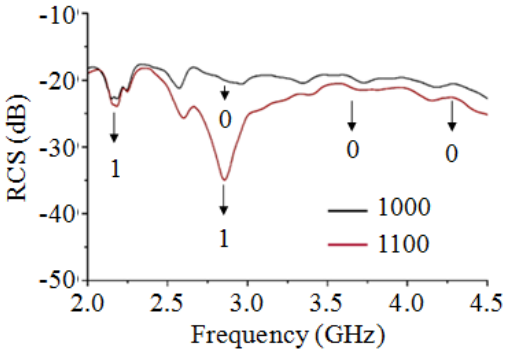

Fig. 3. RCS responses of the frequency-coded chipless RFID tags.

As both the tags employ several EM resonators, to investigate the bandwidth of the resonators is important. In the next section, we analyze the RCS bandwidth of twenty-four resonators, clarifying the design guidelines that lead to enhanced capacity for the frequency-coded chipless RFID.

III. Comparison of the Bandwidth of Resonators

The topology of the EM resonators to be investigated includes a thin strip, step impedance, first-order Z-curve strip, second-order Z-curve strip, dual L strip, S-curve strip, circular slot, half-wave slot, circular split ring, circular loop, dual circular loop, circular loop with a disk, meander strip, C-curve strip, C-curve extended strip, dual-rhombic resonator, second-order Hilbert curve, third-order Hilbert curve, quarter-wave slot, square split ring, square loop, dual square loop and square loop with a disk. Their geometries are depicted in TABLE I. In order to directly attach the tag to an object for item-level tagging, these resonators are printed single-sided and the other side is not metalized.

These resonators are designed to depict a fundamental resonance at 3 GHz. The 3-dB RCS bandwidth of these resonators is evaluated using CST simulation. Additionally, the amplitude of the RCS at 3 GHz is analyzed. The conductor is assigned to be copper, and the substrate is RO4003 (relative permittivity $\varepsilon_r = 3.5$ and loss tangent $\tan\delta = 0.002$). As a result, the 3-dB bandwidth and the amplitude of the RCS are summarized in TABLE I.

TABLE I. COMPARISON OF THE BANDWIDTH FOR TWENTY-FOUR RESONATORS

Resonator	Illustration	Bandwidth (MHz)	RCS (dB)	Resonator	Illustration	Bandwidth (MHz)	RCS (dB)
Thin strip	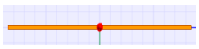	436	–21.6	Meander strip	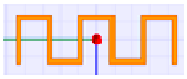	159	–21.4
Step impedance		435	–21.2	C-curve strip #1	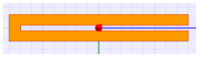	60	–41
1st-order Z-curve strip	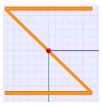	120	–22.2	C-curve strip #2	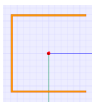	120	–24.4
2nd-order Z-curve strip	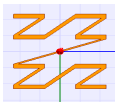	68	–26.1	C-curve extended strip	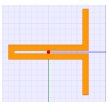	35	–24.4
Dual L strip	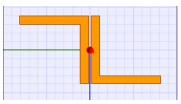	584	–23.6	Dual rhombic	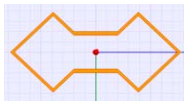	129	–19.4
S-curve strip	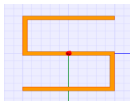	70	–23.0	2nd order Hilbert curve	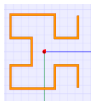	40	–25.8
Circular slot	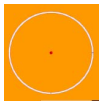	32	–42.7	3rd order Hilbert curve	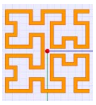	40	–35.2
Half-wave slot		130	–46.2	Quarter-wave slot		25	–34.2
Circular split ring resonator	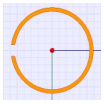	62	–25.6	Square split ring resonator	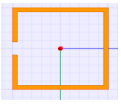	65	–25.6
Circular loop		552	–18.9	Square loop	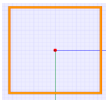	492	–19.3
Dual circular loop		82	–20.7	Dual square loop	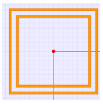	90	–20.6
Circular loop with a disk	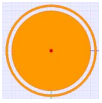	100	–20.2	Square loop with a disk	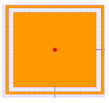	112	–19.8

TABLE I presents the potential of capacity enhancement using these resonators. Although some resonators (such as the circular loop and the dual L strip) have a relatively extensive bandwidth, which causes RCS aliases for two successive frequency slots, several topologies depict the narrowband characteristic. In particular, the circular slot depicts a bandwidth of 32 MHz, and the quarter-wave slot depicts a bandwidth of 25 MHz. These resonators provide the narrowest bandwidth. Additionally, the C-curve extended strip and the second- and third-order Hilbert curve resonators have a bandwidth of less than 45 MHz. These resonators are

recommended for being implemented in the chipless tag, as they can increase the resolution for a chipless RFID system.

IV. Conclusion

In this study, we have provided design guidelines for the resonators that are employed in the chipless RFID tag. The background of the frequency-coded chipless RFID has been illustrated. Based on the requirement of this application, we have designed twenty-four resonators, evaluating the RCS response. It is observed that the quarter-wavelength slot, the circular slot, the C-curve extended strip and the Hilbert-curve resonators depict narrow bandwidths. These resonators have a potential to provide the chipless tag with enhanced capacity. These design rules are expected to provide guidance for future chipless tag development.

Acknowledgment

The authors would like to acknowledge the support from the Ministry of Science and Technology, Taiwan, of Contract MOST 107-2636-E-027-001.

References

[1] S. Härmä, V. P. Plessky, X. Li, and P. Hartogh, "Feasibility of ultra-wideband SAW RFID tags meeting FCC rules," *IEEE Trans. Ultrason., Ferroelect. Freq. Control*, vol. 56, no. 4, pp. 812–820, Apr. 2009.

[2] M. M. Khan, F. A. Tahir, M. F. Farooqui, A. Shamim, and H. M. Cheema, "3.56-bits/cm2 compact inkjet printed and application specific chipless RFID tag," *IEEE Antennas Wireless Propag. Lett*., vol. 15, pp. 1109–1112, 2016.

[3] M. Pöpperl, A. Parr, C. Mandel, R. Jakoby, and M. Vossiek, "Potential and practical limits of time-domain reflectometry chipless RFID," *IEEE Trans. Microw. Theory Techn*., vol. 64, no. 9, pp. 2968–2976, Sep. 2016.

[4] S. Genovesi, F. Costa, A. Monorchio, and G. Manara, "Chipless RFID tag exploiting multifrequency delta-phase quantization encoding," *IEEE Antennas Wireless Propag. Lett*., vol. 15, pp. 738–741, 2015.

[5] C. Feng *et al*., "Angle-based chipless RFID tag with high capacity and insensitivity to polarization," *IEEE Trans. Antennas Propag*., vol. 63, no. 4, pp. 1789–1797, Apr. 2015.

[6] H.-W. Son and C.-S. Pyo, "Design of RFID tag antennas using an inductively coupled feed," *Electron. Lett*., vol. 41, no. 18, pp. 994–996, Sept. 2005.

[7] M. Borgese, F. A. Dicandia, F. Costa, S. Genovesi, and G. Manara, "An inkjet printed chipless RFID sensor for wireless humidity monitoring," *IEEE Sensors J*., vol. 17, no. 15, pp. 4699–4707, Aug. 2017.

[8] A. Vena, E. Perret, and S. Tedjni, "A depolarizing chipless RFID tag for robust detection and its FCC compliant UWB reading system," *IEEE Trans. Microw. Theory Techn*., vol. 61, no. 8, pp. 2982–2994, Aug. 2013.

[9] H. Huang and L. Su, "A compact dual-polarized chipless RFID tag by using nested concentric square loops," *IEEE Antennas Wireless Propag. Lett*., vol. 16, pp. 1036–1039, 2017.

[10] M. Zomorrodi and N. C. Karmakar, "Chipless RFID reader: Low-cost wideband printed dipole array antenna," *IEEE Antennas Propag. Mag*., vol. 57, no. 5, pp. 18–29, Oct. 2015.

[11] A. Vena *et al*., "Design of chipless RFID tags printed on paper by flexography," *IEEE Trans. Antennas Propag*., vol. 61, no. 12, pp. 5868–5877, Dec. 2013.

[12] A. Vena, A. A. Babar, L. Sydänheimo, M. M. Tentzeris, and L. Ukkonen, "A novel near-transparent ASK-reconfigurable inkjet-printed chipless RFID tag," *IEEE Antennas Wireless Propag*. Lett., vol. 12, pp. 753–756, 2013.

[13] D. Betancourt, K. Haase, A. Hübler, and F. Ellinger, "Bending and folding effect study of flexible fully printed and late- stage codified octagonal chipless RFID tags," *IEEE Trans. Antennas Propag*., vol. 64, no. 7, pp. 2815–2823, Jul. 2016.

[14] M. A. Islam and N. C. Karmakar, "Compact printable chipless RFID systems," *IEEE Trans. Microw. Theory Techn*., vol. 63, no. 11, pp. 3785–3793, Nov. 2015.

[15] D. Betancourt *et al*., "Design of printed chipless-RFID tags with QR-code appearance based on genetic algorithm," *IEEE Trans. Antennas Propag*., vol. 65, no. 5, pp. 2190–2195, May 2017.

[16] C. M. Nijas *et al*., "Low-cost multiple-bit encoded chipless RFID tag using stepped impedance resonator," *IEEE Trans. Antennas Propag*., vol. 62, no. 9, pp. 4762–4770, Sep. 2014.

[17] C. M. Nijas *et al.*, "Chipless RFID tag using multiple microstrip open stub resonators," *IEEE Trans. Antennas Propag*., vol. 60, no. 9, pp. 4429–4432, Sep. 2012.

[18] R. S. Nair and E. Perret, "Folded multilayer C-sections with large group delay swing for passive chipless RFID applications," *IEEE Trans. Microw. Theory Techn*., vol. 64, no. 12, pp. 4298–4311, Dec. 2016.

[19] S. Preradovic and N. C. Karmakar, "Design of chipless RFID tag for operation on flexible laminates," *IEEE Antennas Wireless Propag. Lett*., vol. 9, pp. 207–210, 2010.

[20] F. Costa, S. Genovesi, and A. Monorchio, "A chipless RFID based on multi-resonant high-impedance surfaces*," IEEE Trans. Microw. Theory Techn*., vol. 61, no. 1, pp. 146–153, Jan. 2013.

[21] F. Costa, S. Genovesi, and A. Monorchio, "Chipless RFIDs for metallic objects by using cross polarization encoding," *IEEE Trans. Antennas Propag*., vol. 62, no. 8, pp. 4402–4407, Aug. 2014.

[22] J. G. D. Hester and M. M. Tentzeris, "Inkjet-printed flexible mm-wave van-atta reflectarrays: A solution for ultralong-range dense multitag and multisensing chipless RFID implementations for IoT smart skins," *IEEE Trans. Microw. Theory Techn.,* vol. 64, no. 12, pp. 4763–4773, Dec. 2016.